

# Drying behavior of hydratable alumina-bonded refractory castables

Fábio A. Cardoso, Murilo D.M. Innocentini, Marcela F.S. Miranda,  
Fernando A.O. Valenzuela, Victor C. Pandolfelli\*

*Department of Materials Engineering, UFSCar, Federal University of São Carlos, Via Washington Luiz, km 235, 13565-905,  
São Carlos, SP, Brazil*

Received 9 January 2003; received in revised form 2 April 2003; accepted 13 April 2003

## Abstract

The drying behavior of a hydratable alumina-bonded (HAB) refractory castable was evaluated by thermogravimetric tests and compared with an ultra-low cement composition (CAC). The key properties of monolithic refractory dry-out performance, such as fluid permeability and mechanical strength, were also determined. The results showed significant differences among the drying profiles ascribed to the distinct hydrated binding phases, which affect the castables' physical properties to a differing extent. The consequences of these features on the explosive spalling tendencies of the compositions are discussed.

© 2003 Elsevier Ltd. All rights reserved.

*Keywords:* Al<sub>2</sub>O<sub>3</sub>; Ca-free hydraulic binder; Drying; Mechanical Properties; Refractories

## 1. Introduction

Substantial advances in monolithic refractory technology over the last decades have led not only to important innovations in castable preparation and application processes<sup>1</sup> but also to significant improvements in product performance, in response to the constantly increasing service conditions imposed mainly by the steel and foundry industries. In this context, reductions in the CaO content of high-alumina and alumina-silica formulations have been sought to enhance thermomechanical resistance by diminishing the formation of less refractory phases,<sup>1–3</sup> which, in turn, have led to the development of ultra-low cement and no-cement castables, as well as Ca-free hydratable alumina binders.<sup>4</sup>

Because ultra-low binding, low-water containing castables are commonly produced with fine reactive powders and have improved particle-packing design, they generally display low porosity and permeability levels, which has led to spalling problems during the dewatering stage. Therefore, several studies<sup>5–9</sup> have focused on the drying behavior and related features of the widely used calcium aluminate cement (CAC) based monolithics, whereas little research has involved the

dry-out and explosive spalling behavior of hydratable alumina-bonded (HAB) refractory castables. The lack of detailed data, allied to the evidence from industry, which reports that this type of composition presents an even more complex dewatering process than CAC containing products, may have contributed to restrict the application of Ca-free hydratable alumina binders.

## 2. Hydratable alumina as a refractory binder

Hydratable aluminas are generally produced via flash calcination of gibbsite, resulting mainly in a high-surface area transition phase called rho-alumina.<sup>10,11</sup> The binding ability of rho-alumina derives from its particular characteristic of undergoing rehydration when in contact with water (or water vapor). During hydration, a thick layer of gel is formed, part of the gel subsequently crystallizing into traces of boehmite and major quantities of bayerite.<sup>12,13</sup> The remaining gel phases have been identified as boehmite gel or pseudo-boehmite (a poorly crystallized boehmite), together with a totally amorphous gel, and may represent up to 60% of the final hydrated phases, depending on the hydration temperature and pH.<sup>13,14</sup> Interlocking bayerite crystals and gel confer green mechanical strength on the refractory structure by filling pores and interfacial defects and

\* Corresponding author.

*E-mail address:* [vicpando@power.ufscar.br](mailto:vicpando@power.ufscar.br) (V.C. Pandolfelli).

by forming honeycomb structures on the surface of aggregates,<sup>12</sup> attaching adjacent grains to each other and to the surrounding matrix.

On the other hand, calcium aluminate cement technology relies on the hydration capacity, primarily of CA<sup>1</sup> and secondly of CA<sub>2</sub>, to rapidly yield various calcium aluminate hydrated phases (CAH<sub>10</sub>, C<sub>2</sub>AH<sub>8</sub> and C<sub>3</sub>AH<sub>6</sub>) and alumina hydrates (gibbsite and gel).<sup>15–17</sup> These hydrated phases are strongly influenced by the curing temperature, varying from CAH<sub>10</sub> and alumina gel ( $T < 15$  °C) to C<sub>3</sub>AH<sub>6</sub> and crystalline AH<sub>3</sub> ( $T > 40$  °C),<sup>15–17</sup> leading to diverse spalling tendencies in similar CAC compositions cured at different temperatures. When minor quantities of binder are employed, few or no modifications are needed in the formulation, mixing and application practices when replacing CAC with HAB.<sup>4</sup> However, the considerable differences between the hydraulic binding phases may affect the castables' physical properties unequally, thereby causing distinct drying behaviors.

Castable dewatering profiles are very difficult to assess due to the large size of refractory pieces in real situations. Therefore, the drying process is optimized based entirely on pragmatism and on trial and error. This has prevented refractory drying schedules from keeping up with the major advances and innovations achieved in other areas of monolithics processing, causing dry-out to continue being a costly and time-consuming step. Precise mass loss and temperature data, obtained by an accurate thermogravimetric technique applied to small castable specimens, may be extrapolated to industrial drying situations, aiding refractory producers and consumers to design suitable heating curves. These schedules allow not only for the safe removal of water and preservation of the products' physical integrity, but also the reduction of turnaround times in drying chambers (for pre-cast pieces) and linings (for in-situ applications).

Considering these circumstances, the present work investigates the drying behavior of HAB castables, highlighting their properties (regarding the drying performance) compared with those of CAC castables. For this purpose, permeability and mechanical measurements, along with several thermogravimetric (TG) tests, were conducted on compositions based on the various hydraulic binders. The reasons for the particular explosive spalling tendency of HAB formulations were also investigated.

### 3. Experimental procedure

Two castable compositions (98 wt.% alumina and 2 wt.% binder) were designed based on different hydraulic binding agents, with particle size distributions adjusted

to theoretical curves based on Andreasen's packing model, with a distribution coefficient ( $q$ ) of 0.21. The mixtures were composed of matrix powders (calcined A1000 SG and A3000 FL aluminas, 23 wt.%,  $d_{\max} < 100$  μm), aggregate grains (white fused aluminas, grades 4/10, 8/20, 10/36, 20/40 and 200F, 75 wt.%,  $d_{\max} < 4.5$  mm) and hydraulic binder: calcium aluminate cement (CA-14) for the CAC composition and hydratable alumina (Alphabond-200) for the HAB composition. Both castables were mixed with 4.50 wt.% of water (dry basis) and dispersed with citric acid (LabSynth, Brazil). The alumina and binder raw materials were supplied by Alcoa Brazil and USA.

The castable compositions were molded into 4.0 cm diameter by 4.0 cm high cylinders for the drying and the mechanical tests, and into 7.5 cm diameter by 2.2 cm thick disks for permeability measurements. The samples used to measure the actual sample temperature during the drying tests were molded with a K-type thermocouple located at the center of the cylinder's upper surface (2 mm depth). All the bodies were cured in the molds at 50 °C for 48 h.

The drying tests were performed in a TG device composed of an electric furnace (with no forced air stream) coupled to a digital scale. The temperature and mass data were computer-recorded at 5-s intervals throughout the tests. Results correlating the sample's temperature with its mass loss profile were obtained using data from two tests conducted with the same heating program on specimens of the same batch (one for mass data and the other for temperature acquisition). Basically, two different types of heating schedules were applied, the first consisting of continuous heating from room temperature to 800 °C at different rates (10 and 20 °C/min). The second procedure was based on a dwell time at a constant temperature, with the sample heated from room temperature to 110 °C at a rate of 5 °C/min and then held at that temperature for 500 min (sufficient time for constant mass to be reached).

The parameters analyzed in the drying tests were  $W_d$  and  $dW_d/dt$ , representing the cumulative fraction of water loss and the specimen's drying rate, respectively.  $W_d$  was calculated as:

$$W_d(\%) = 100 \times \left( \frac{M_o - M_f}{M_f} \right) \quad (1)$$

where  $M$  is the instantaneous mass recorded at time  $t_i$  during the heating stage,  $M_o$  is the initial mass and  $M_f$  is the final mass of the tested sample. In this study,  $W_d$  varied from 0 to 4.5%, which corresponded to the total casting water added ( $W_d = W_{df}$  when  $M = M_f$ ). The experimental drying rates  $dW_d/dt$  were obtained by the derivation of  $W_d$  curves as a function of time.

In order to assess the dehydration profiles of the binding phases, specimens of each composition were dried in silica gel prior to the thermogravimetric tests

<sup>1</sup> Stands for: C = CaO; A = Al<sub>2</sub>O<sub>3</sub>; H = H<sub>2</sub>O.

(specimens referred to as CAC–MF<sup>2</sup> and HAB–MF). Samples for permeability and mechanical evaluations were also previously dried in silica gel. In this case, however, the moisture was removed primarily to prevent any influence of free water on the measurements.

Room temperature permeability tests were performed on two bodies for each composition. The experiments evaluated the easiness of airflow through the sample's thickness by measuring the exit air velocity in response to the variations of the inlet pressure applied. The permeability constants  $k_1$  and  $k_2$  were obtained by fitting the experimental data using Forchheimer's equation.<sup>2</sup>

$$\frac{P_1^2 - P_0^2}{2PL} = \left(\frac{\mu}{k_1}\right)v_s + \left(\frac{\rho}{k_2}\right)v_s^2 \quad (2)$$

where  $P_1$  and  $P_0$  are the absolute inlet and outlet air pressures, respectively;  $v_s$  is the fluid velocity;  $L$  the sample thickness;  $\mu$  the fluid viscosity; and  $\rho$  the fluid density. The parameters  $k_1$  and  $k_2$  are, respectively, the Darcian and non-Darcian permeability constants.

Mechanical tests were conducted according to the ASTM C496-90 standard (Splitting Tensile Strength of Cylindrical Concrete Specimens) in a MTS device (MTS Systems, Model 810, Minneapolis, MN) on six dried samples of each castable composition.

## 4. Results and discussion

### 4.1. Physical properties

Table 1 lists the results of the main physical properties relating to the drying characteristics of HAB and CAC compositions. The permeability parameters ( $k_1$  and  $k_2$ ) were strongly affected by the kind of binder used, while the mechanical strength was influenced to a lesser extent.

The CAC castable displayed a six-fold greater  $k_1$  and a 115-fold greater  $k_2$  than the HAB samples. This substantial difference between the castables' permeability levels resulted from the characteristics of the hydrated binding phases present in each type of refractory. The binding phases in the CAC composition were exclusively  $C_3AH_6$  and gibbsite (as it was cured at 50 °C),

whereas in the HAB samples, bayerite was the major crystalline phase, in addition to gel phases (pseudo-boehmite and totally amorphous gel). It is worth noting that pH values exceeding 9.5 were found to strongly favor the formation of gel during rho-alumina hydration,<sup>14</sup> and the measured pH of the HAB formulation in this work indicated a variation from 9.40 (immediately after mixing) to 9.85 (after 90 min). Therefore, gel phases probably represent a significant fraction of the hydrated phases in HAB castables.

Gelatinous alumina phases are very efficient in clogging pores and interfacial defects,<sup>9</sup> causing severe obstructions to internal fluid flow. Moreover, the particular features of the binders' particle size distributions have been reported<sup>2</sup> to influence the thickness of the porous zone at the interfaces. The smaller particles of Alphasbond 200 ( $d_{50}=2.6 \mu\text{m}$ ,  $d_{90}=5.4 \mu\text{m}$ ) provided better packing around the aggregates than CA-14 particles ( $d_{50}=13 \mu\text{m}$ ,  $d_{90}=50 \mu\text{m}$ ), since the former binder was assumed to exert a less intense wall effect than the latter. After hydration, these regions, which already displayed a denser structure (compared to CAC), were filled with gel, resulting in the significant difference between the castables' permeabilities.

Based on the lower permeability of HAB bodies, their porosity could reasonably be presumed to be lower, implying a higher mechanical strength than that of the cement-based composition. However, the results of this work revealed that the CAC castable was 62.4% stronger than the HAB formulation. This fact possibly has to do with the texture of hydrated binding products and their intrinsic mechanical strength. Further investigations are required to clarify this effect.

### 4.2. Drying behavior

Fig. 1a illustrates the drying profiles of CAC and HAB castables in response to a 10 °C/min heating rate. Curves (i) and (ii) show the drying rates ( $dW_d/dt$ ) as a function of the sample temperature for the as-cured CAC and HAB specimens. Both curves present two main peaks corresponding to the evaporation (from room temperature to 100 °C) and ebullition of free water, respectively.<sup>8</sup> The second peak also includes the dehydration of a considerable portion of the binding phases (from 100 to 250–350 °C), revealed by curves (iii) and (iv), which refer to CAC and HAB moisture-free samples. Additionally, the water losses occurring after the second main peak relate to the final stages of binding phase dehydration, as evidenced by the very similar dewatering behavior of as-cured and moisture-free samples within the temperature ranges of 250–600 °C for CAC and 350–600 °C for HAB.

The drying profiles of the MF-samples indicated that dehydration of the diverse binding phases of CAC and HAB occurred in the same temperature range. However,

Table 1  
Permeability constants ( $k_1$  and  $k_2$ ) and mechanical strength ( $\sigma$ ) of the castables based on different hydraulic binders cured at 50 °C

Castable Type	$k_1$ ( $10^{-16} \text{ m}^2$ )	$k_2$ ( $10^{-15} \text{ m}$ )	$\sigma$ (MPa)
CAC	$2.36 \pm 0.46$	$19.6 \pm 3.68$	$2.03 \pm 0.29$
HAB	$0.38 \pm 0.07$	$0.17 \pm 0.02$	$1.25 \pm 0.17$

<sup>2</sup> MF, moisture free.

the former composition showed three main dehydration peaks, depicted in curve (iii), while the latter showed a more continuous band of water loss, evidenced in curve (iv). The first two peaks (177 and 230 °C) in the CAC–MF curve were associated with crystalline gibbsite, which loses most of its molecules as water between 180 and 300 °C,<sup>10,19</sup> although the most intense mass loss occurs at 230 °C.<sup>17</sup> The third peak, appearing at around 300 °C, was probably caused to some extent by gibbsite dehydration but primarily by the decomposition of  $C_3AH_6$  crystals between 240 and 370 °C.<sup>16,17</sup> The next mass loss, at temperatures above 400 °C, was inferred for the final stages of gibbsite decomposition.<sup>10</sup> On the other hand, the drying pattern of the HAB binding phases was composed of different dehydration effects presenting two small broad peaks (195 and 285 °C). Pseudoboehmite decomposes in two temperature ranges, mainly from 100 to 180 °C and, to a lesser degree, at 400–500 °C,<sup>18</sup> while totally amorphous alumina gel probably dries at around 100 °C.<sup>15,17</sup> Crystalline bayerite and boehmite hydrate, respectively, at around 300 °C and between 450 and 550 °C.<sup>10,12,18</sup> The presence of the abovementioned crystalline phases was confirmed by X-ray analysis.

A comparison of curves (i) and (ii) in Fig. 1 reveals that, due to the considerable difference between the castables' permeabilities, the intensity of the HAB

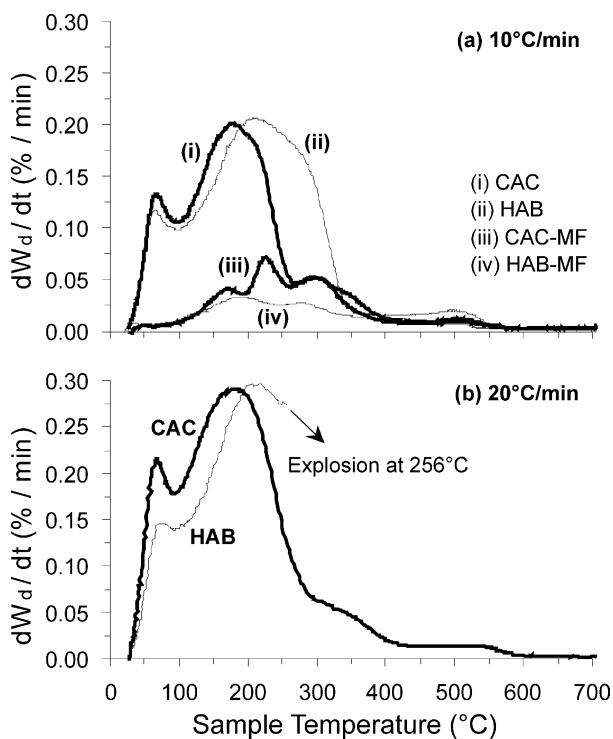


Fig. 1. Drying behavior of green castables bonded with CAC and HAB subjected to continuous heating: (a) Rate of 10 °C/min from room temperature up to 800 °C. Curves (iii) and (iv) refer to moisture free (MF) samples. (b) A more aggressive heating rate (20 °C/min) was applied to evaluate the explosive spalling occurrence.

evaporation peak was lower than that of the CAC drying profile, indicating that a larger amount of free water remained available for vapor pressurization during the ebullition stage. The low permeability of the HAB samples not only restricted the evaporation process but also affected the second peak, causing it to shift to higher temperatures as the release of steam was adversely affected. Hence, greater pressure gradients (i.e., higher temperatures) were required to expel the water vapor from the bulk of the solid at the same rate as from the CAC bodies. The HAB ebullition peak occurred at 36 °C above that of the respective CAC composition (215 and 179 °C), indicating a drying condition involving a greater risk of explosive spalling, since this increase in the peak temperature can double the maximum vapor pressure ( $P_V$ ) from 1.0 to 2.0 MPa, according to Antoine's equation,<sup>8</sup> as shown in Fig. 2.

The level of  $P_V$  at 215 °C, calculated by Antoine's equation (2.0 MPa) in the aforementioned situation, was higher than the measured mechanical strength of the HAB castable (1.25 MPa). Nevertheless, it should be noted that the castable's structure was not impermeable, which meant that steam was continuously released from the solid during heat-up, causing the body's internal pressure to be lower than the  $P_V$  predicted by Antoine. Explosion occurs when the pressure developing inside the castable structure—caused by steam being generated faster than it can be released from the bulk of the solid—reaches the body's maximum tensile strength. Because vapor generation and heating rates are directly correlated, explosive spalling did not occur at a 10 °C/min ramp, but the application of a higher rate, as in Fig. 1b, resulted in explosive spalling.

When subjected to a 20 °C/min heating rate, both specimens presented higher peaks than at 10 °C/min, since the velocity of steam generation was greater and, consequently, the likelihood of pressurization as well. Moreover, in this case, the HAB drying profile was critically influenced by the permeability, further restricting the evaporation stage and dangerously removing a larger quantity of free-water at higher temperatures, since

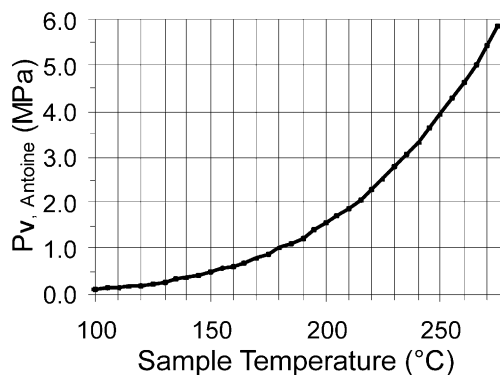


Fig. 2. Maximum vapor pressure as a function of temperature according to Antoine's equation.

the ebullition peak also shifted further upward. This resulted in strong explosive spalling at 256 °C, accompanied by the release of a large amount of energy, as evidenced by the “pulverization” of the HAB sample. As Fig. 2 illustrates, the maximum vapor pressure at 256 °C is 4.4 MPa, which is higher than the mechanical resistance of the HAB castable. Therefore, the important features of Antoine’s relationship are both the absolute value of the maximum calculated  $P_v$  and the exponential increase of pressurization potential as a function of the temperature. The shifting effect caused by structures with low permeability can be extremely dangerous in terms of explosive spalling, because a slight increase in temperature above 150 °C causes a major rise in pressure.

On the other hand, the CAC sample, which had a much higher permeability and considerably greater mechanical strength than HAB, did not suffer explosive spalling since it released vapor more easily (which was confirmed by the higher  $dW_d/dt$  in the evaporation stage and the lower temperature of the ebullition stage) and its stronger bonds withstood the mechanical stresses.

The most commonly employed practical solution for the safe dry-out of refractory castables is based on the application of heating schedules designed with dwell times at different temperatures to separately remove physically and chemically bonded water contents. These schedules are considerably less harmful to a product’s integrity than rapid continuous heating but are more time-consuming and costly. According to this methodology, Fig. 3 depicts the drying behavior of HAB and CAC castables when subjected to a constant-temperature drying procedure. The very low permeability displayed by HAB bodies negatively affected the drying process, although there was no significant pressure build-up but a considerable delay for the complete removal of moisture compared to the CAC sample. As a result, the HAB castable took 66.6% more time to lose 95% of its total free-water content than the CAC-based sample.

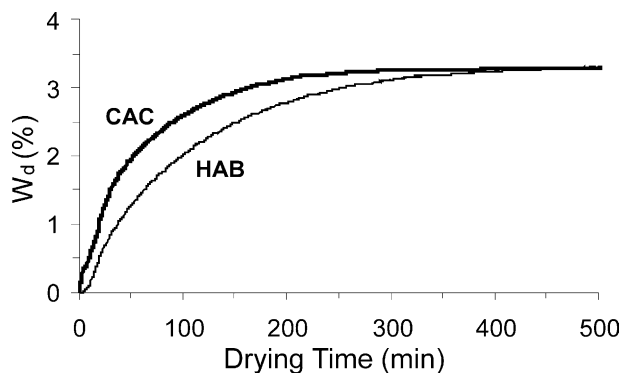


Fig. 3. Drying behavior of castables subjected to a dwell time of 500 minutes at 110 °C.

The optimization of HAB composition drying schedules is limited by the risk of pressurization (when faster heating rates are applied) and by time-consuming, low-risk moisture removal (when lengthy constant-temperature treatments are applied). The use of this class of binder will depend on a cost–benefit relationship between the time/energy cost of the dewatering process and thermomechanical improvements.

## 5. Conclusions

The spalling tendency observed in the HAB refractory castable originated from its low permeability, which was ascribed to gel-like phases that make up a considerable portion of the hydrated phases in Ca-free specimens. The consequence of these gel-like phases on the drying behavior was to shift the removal of free water to higher temperatures (than in CAC bodies) and, consequently, to increase the steam pressure and the likelihood of explosive spalling under fast continuous heating. When subjected to a constant-temperature drying procedure, the HAB sample took considerably longer than the cement-based body to lose the physically absorbed water content. The CAC castable was found to be much more permeable and considerably stronger than HAB, releasing vapor more easily and showing a stronger structure to withstand the pressure build-up, which explains the low tendency for explosive spalling of cement containing compositions cured at 50 °C.

## Acknowledgements

The authors would like to thank the Brazilian research-funding institutions CAPES and FAPESP, and also ALCOA S.A. and MAGNESITA S.A., for supporting this work.

## References

1. Lee, W. E. and Moore, R. E., Evolution of in situ refractories in the 20th Century. *J. Am. Ceram. Soc.*, 1998, **81**(6), 1385–1410.
2. Innocentini, M. D. M., Pardo, A. R. F., Menegazzo, B. A., Bitencourt, L. R. M., Rettore, R. P. and Pandolfelli, V. C., Permeability of high-alumina refractory castables based on various hydraulic binders. *J. Am. Ceram. Soc.*, 2002, **85**(6), 1517–1521.
3. Studart, A. R., Zhong, W. and Pandolfelli, V. C., Rheological design of zero-cement self-flow castables. *Am. Ceram. Soc. Bull.*, 1999, **78**(5), 65–72.
4. Vance, M. W. and Moody, K. J., Use of hydratable alumina binders in refractory compositions and related applications. Presented at the 97th Annual Meeting of the American Ceramic Society, 1995, Cincinnati.
5. Gitzen, W. H. and Hart, L. D., Explosive spalling of refractory castables bonded with calcium aluminate cement. *Am. Ceram. Soc. Bull.*, 1961, **40**(8), 503–507 510.

6. Velez, M., Erkal, A. and Moore, R. E., Computer simulation of the dewatering of refractory concretes walls. *Journal of the Technical Association of Refractories, Japan*, 2000, **20**(1), 5–9.
7. Schmitt, N., Hernandez, J. F., Lamour, V., Berthaud, Y., Meunier, P. and Poirier, J., Coupling between kinetics of dehydration, physical and mechanical behaviour for high alumina castable. *Cement and Concrete Research*, 2000, **30**, 1597–1607.
8. Innocentini, M. D. M., Cardoso, F. A., Akyioshi, M. M. and Pandolfelli, V. C., Drying stages during the heat-up of high-alumina, ultra-low cement refractory castables, *J. Am. Ceram. Soc.* (accepted for publication).
9. Cardoso, F. A., Innocentini, M. D. M., Akyioshi, M. M. and Pandolfelli, V. C., Effect of curing time on the properties of CAC bonded refractory castables. *J. Eur. Ceram. Soc.*, (accepted for publication).
10. Wefers, K. and Mishra, C., *Oxides and Hydroxides of Aluminum. Alcoa Technical Paper No. 19*. Aluminum Company of America, Pittsburgh, PA, 1987.
11. Ma, W. and Brown, P. W., Mechanisms of reaction of hydratable aluminas. *J. Am. Ceram. Soc.*, 1999, **82**(2), 453–456.
12. Hongo, Y.,  $\rho$ -alumina bonded castable refractories. *Taikabutsu Overseas*, 1988, **9**(1), 35–38.
13. Mista, W. and Wrzyszczyk, J., Rehydration of transition aluminas obtained by flash calcination of gibbsite. *Thermochimica Acta*, 1999, **331**, 67–72.
14. Vaidya, S. D. and Thakkar, N. V., Effect of temperature, pH and ageing time on hydration of rho alumina by studying phase composition and surface properties of transition alumina obtained after thermal dehydration. *Materials Letters*, 2001, **51**, 295–300.
15. Parker, K. M. and Sharp, J. H., Refractory calcium aluminate cements. *Trans. J. British Ceram. Soc.*, 1982, **81**, 35–42.
16. Maczura, G., Hart, L. D. and Heilich, R. P., Refractory cements. *Ceramic Proceedings*, The American Ceramic Society, Inc., 1983, p. 11.
17. Nishikawa, A., Technology of monolithic refractories. *Plibrico Japan CO. Ltd.*, Tokyo, Japan, 1984, pp. 83–170.
18. Vaidya, S. D. and Thakkar, N. V., Study of phase transformations during hydration of rho alumina by combined loss on ignition and X-ray diffraction technique. *Journal of Physics and Chemistry of Solids*, 2001, **62**, 977–986.